

## Supporting Information

### **Activating the high-potential $V^{4+}/V^{5+}$ redox couple for an advanced NASICON sodium-ion cathode**

Miaomiao Wang,<sup>a</sup> Lin Zhu,<sup>a</sup> Shuang Xiang,<sup>a</sup> Xiaobing Huang,<sup>b</sup> Huanhuan Li,<sup>c</sup> Haiyan Wang,<sup>a</sup> Yougen Tang,<sup>a</sup> Dan Sun,<sup>a\*</sup>

- a. Hunan Provincial Key Laboratory of Chemical Power Sources, College of Chemistry and Chemical Engineering, Central South University, Changsha, 410083, P. R. China.  
E-mail: sundan4330@csu.edu.cn
- b. College of Chemistry and Materials Engineering, Hunan University of Arts and Science, Changde 415000, Hunan, China.
- c. School of Chemistry and Chemical Engineering, Henan Normal University, Xinxiang 453007, P. R. China

## Experimental Section

### Material Preparation

The NVCTP-0, NVCTP-2, and NVCTP-4 composites were synthesized using a spray drying technique followed by a post-annealing process. All chemicals were used without further purification. The preparation method of the precursor solution is as follows: First, vanadium (IV)oxy acetylacetonate ( $C_{10}H_{14}O_5V$ ), tetrabutyl titanate ( $C_{16}H_{36}O_4Ti$ ) and chromic nitrate ( $Cr(NO_3)_3 \cdot 9H_2O$ ) are dissolved in 70 ml ethanol solution according to the stoichiometric ratio and vigorous stirring at  $80^\circ C$ . The solution was supplemented with 6.3 g of citric acid ( $C_6H_8O_7$ ) as a chelating agent and carbon source. Sodium acetate ( $C_2H_3NaO_2$ ) and phosphoric acid ( $H_3PO_4$ ) were sequentially added into the mixed solution formed above. The precursor solution was then treated with spray drying, and the inlet temperatures were set to  $170^\circ C$ . Finally, the dried precursor was followed by annealing at  $800^\circ C$  for 5 h in a tube furnace with Ar/ $H_2$  (95:5 vol: vol) atmosphere. NVCTP-0 is prepared by a similar approach except without adding  $Cr(NO_3)_3 \cdot 9H_2O$ .

### Material Characterizations

The chemical composition and crystal structure of the resulting materials were analyzed using X-ray diffraction (XRD, Rigaku/Ultima IV) and refined by Rietveld with the GSAS software. The property analyses of the carbon layer were undertaken on a laser micro-Raman spectrometer (Raman, Renishaw/inVia Reflex) with a laser wavelength of 532 nm, and the carbon contents were further tested by a thermogravimetric analyzer (TGA, Henven/HCT-1) from  $30^\circ C$  to  $800^\circ C$  with a ramping rate of  $10^\circ C \text{ min}^{-1}$  in air. The specific calculation criterion of carbon content is based on the mass loss of between 300 and  $550^\circ C$ , corresponding to the decomposition temperature of carbon in the air.<sup>1</sup> X-ray photoelectron spectroscopy (XPS, Thermo Fisher Scientific/ESCALAB250Xi) was performed to confirm the valence state of transition metals. The morphologies and microstructure images of the synthesized cathodes were observed by scanning electron microscope (SEM, JEOL/JSM-7610FPlus) and transmission electron microscope (TEM, JEM-2100F).

### Electrochemical Measurements

The electrochemical performance experiments were carried out by assembling 2016-type coin cells in an Argon-filled glove box. Using NVCTP-x as working electrodes, sodium metal as counter electrodes, and glass fiber filters as separators. The electrolyte was 1M  $NaClO_4$  dissolved in the mixed

solvent of propylene carbonate (PC) and 5% fluoroethylene carbonate (FEC) additive. To prepare a typical half-cell, the active material, Super P, and polyvinylidene fluoride (PVDF) were mixed in N-methyl-2-pyrrolidone (NMP) solvent at a mass ratio of 70:20:10. The obtained slurry was uniformly coated onto an Al foil and dried at 80°C under vacuum over 6 h. Afterward, the cathode was cut into circular electrodes (12 mm in diameter), and the loading mass of the active material was about 1.5-2.0 mg cm<sup>-2</sup>. To demonstrate the practical feasibility, CR2025 coin cells were further assembled using commercial hard carbon (HC, Kureha Carbotron P) as the anode and NVCTP-2 as the cathode. HC electrode was prepared by mixing with HC (92 wt%), super P (3 wt%), and CMC-SBR (5 wt%) in water followed by coating on Cu foil. To complete the presodiation process, the HC anode wet with the electrolyte was kept in contact with the metallic sodium for approximately 2 h. Notably, the loading of the NVCTP-2 electrode is approximately 1.5 times that of the HC electrode to match the capacity of full cells.

All assembled cells were aged over 6 h before electrochemical measurements. Galvanostatic charge-discharge (GCD) tests between 1.5-4.3 V (vs Na<sup>+</sup>/Na) were carried out on a Neware CT-3008W battery testing system. The parameters of the galvanostatic intermittent titration technique (GITT) were set with a current pulse duration of 0.5 h at 20 mA g<sup>-1</sup> and a further interval time of 2 h. Cyclic voltammetry (CV) curves were recorded on the CHI660e electrochemical workstation.

### **Calculation methods**

The DFT method, as implemented in the Vienna ab initio Simulation Package (VASP), was utilized for all calculations. The ion-electron interaction was handled via the projector augmented wave (PAW) scheme. To further enhance the description of d orbitals in transition metals, we employed the GGA+U method (U values for V, Ti and Cr are 4.2, 4.0 and 3.7 eV, respectively). The plane-wave energy cutoff and the force convergence criterion were set to 500 eV and 0.02 eV Å<sup>-1</sup> respectively.

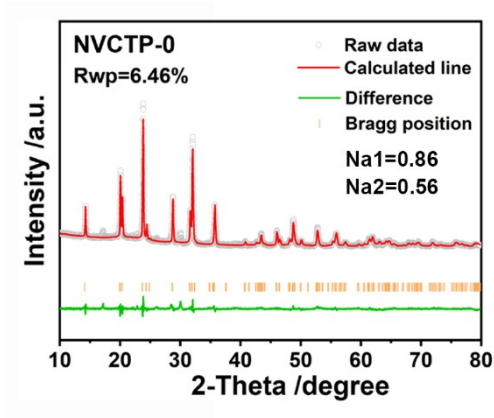


Fig. S1. XRD Rietveld refinement of NVCTP-0 sample.

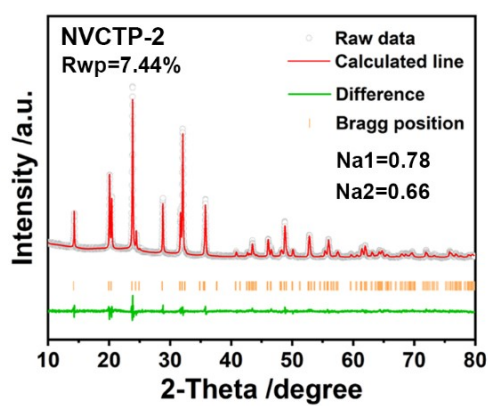


Fig. S2. XRD Rietveld refinement of NVCTP-2 sample.

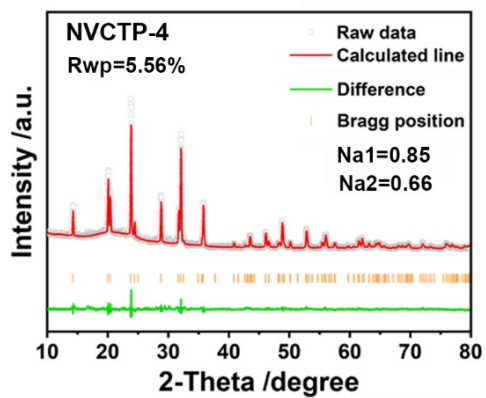


Fig. S3. XRD Rietveld refinement of NVCTP-4 sample.

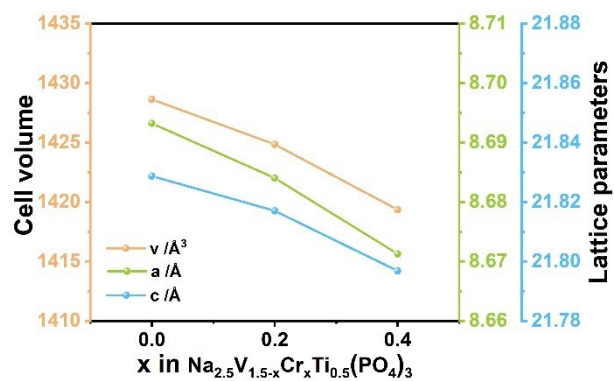


Fig. S4. Cell volume and Lattice parameter variation of NVCTP-x samples.

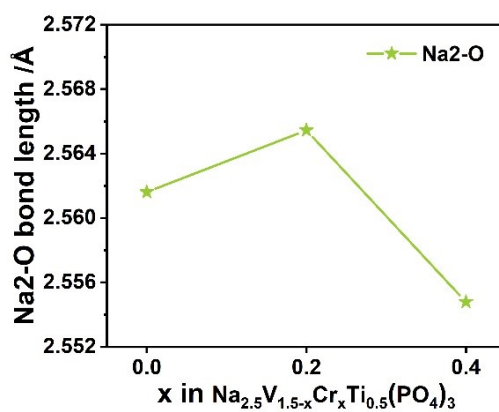


Fig. S5. Bond length of Na2-O in NVCTP-x samples.

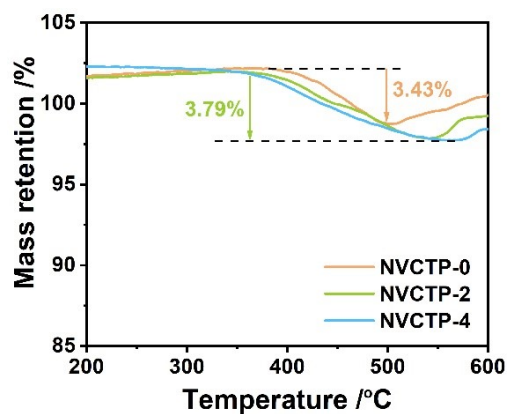
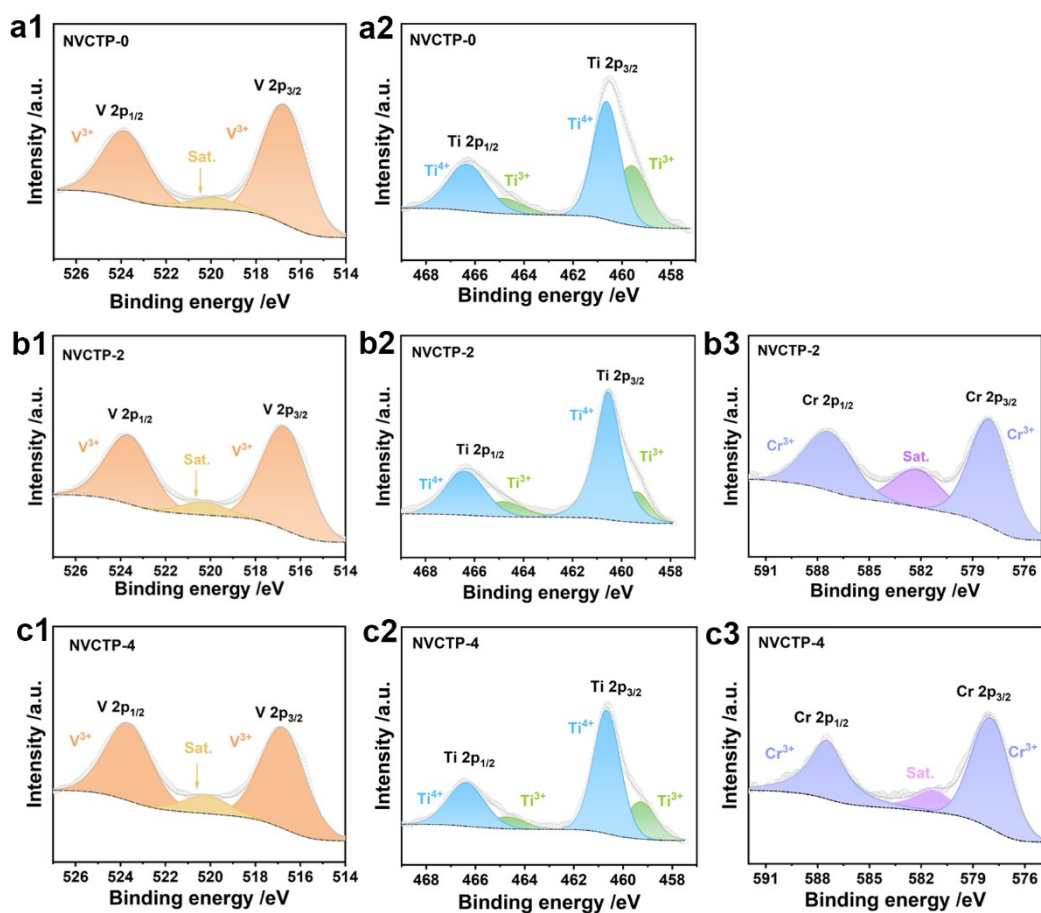
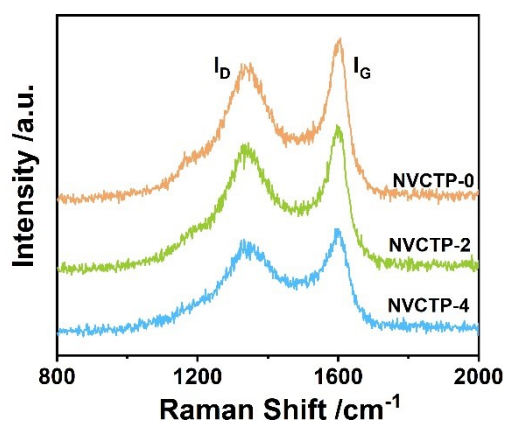


Fig. S6. TG curves of NVCTP-0, NVCTP-2, and NVCTP-4 samples.



**Fig. S7.** High-resolution spectra of V 2p, Ti 2p and Cr 2p for (a) NVCTP-0, (b) NVCTP-2 and (c) NVCTP-4 samples.



**Fig. S8.** Raman spectra of NVCTP-0, NVCTP-2, and NVCTP-4 samples.

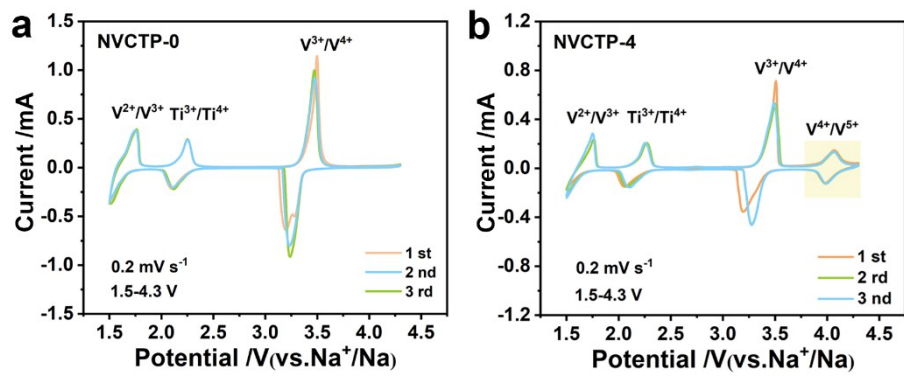


**Fig. S9.** CV curves of (a) NVCTP-0 and (b) NVCTP-4 electrodes.

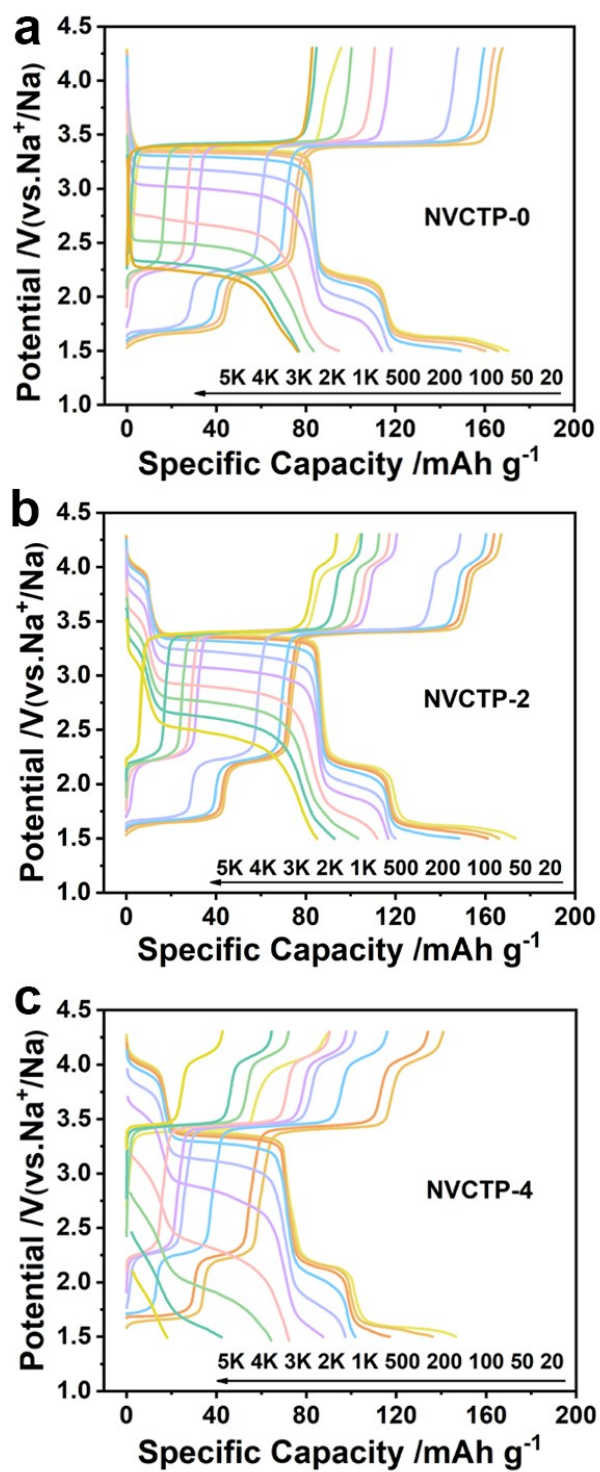


**Fig. S10.** The GCD curves of (a) NVCTP-0, (b) NVCTP-2 and (c) NVCTP-4 cathodes from 20 to

5000 mA g<sup>-1</sup>.



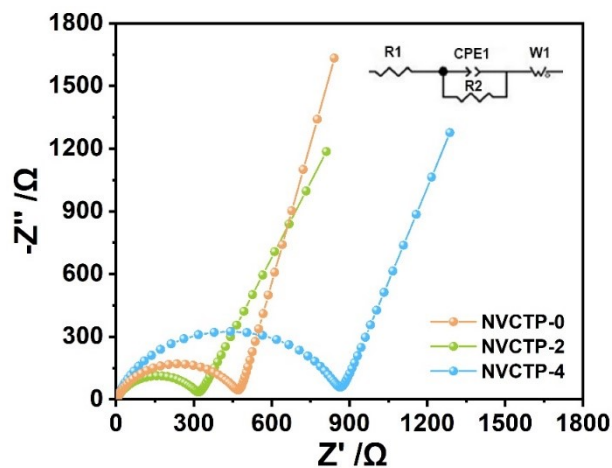


**Fig. S11.** EIS spectra of NVCTP-0, NVCTP-2 and NVCTP-4.

The Nyquist plots consist of a semicircle in the high-frequency region, which corresponds to the charge transfer resistance ( $R_{ct}$ ), and a sloping line relating to the Warburg impedance ( $Z_w$ ) in the low-frequency region.<sup>2,3</sup> The inset shows a characteristic EIS equivalent circuit fitting that includes an electrolyte resistor ( $R_1$ ), a charge transfer resistor ( $R_2$ ), and a constant phase angle element (CPE).<sup>4</sup>

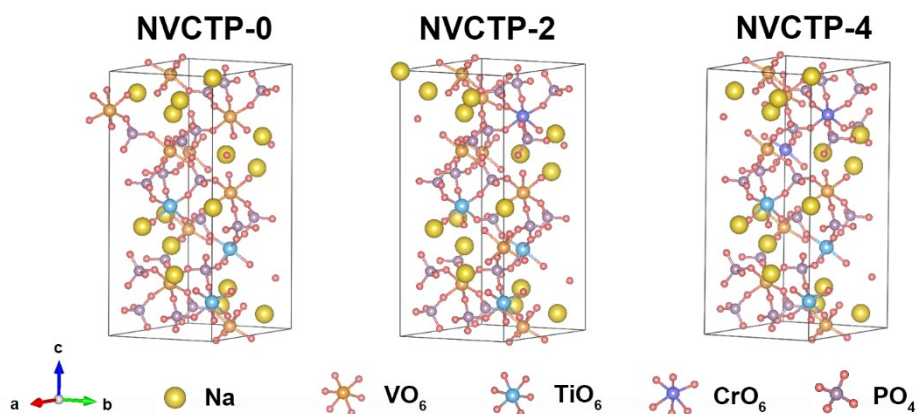


**Fig. S12.** Optimized crystal structure of NVCTP-0, NVCTP-2 and NVCTP-4.

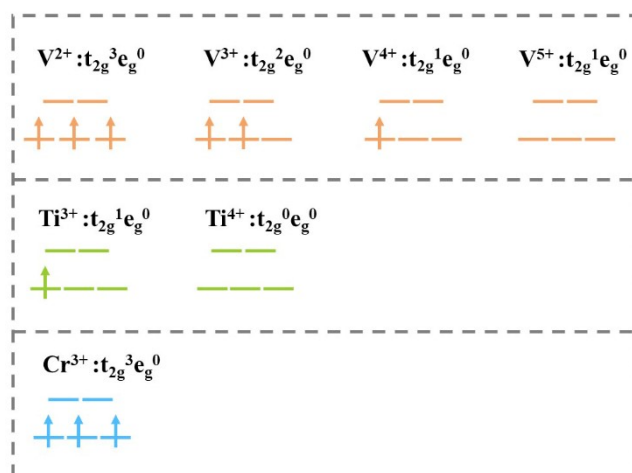


Fig. S13. Schematic view of the electronic configurations of transition-metal ions.

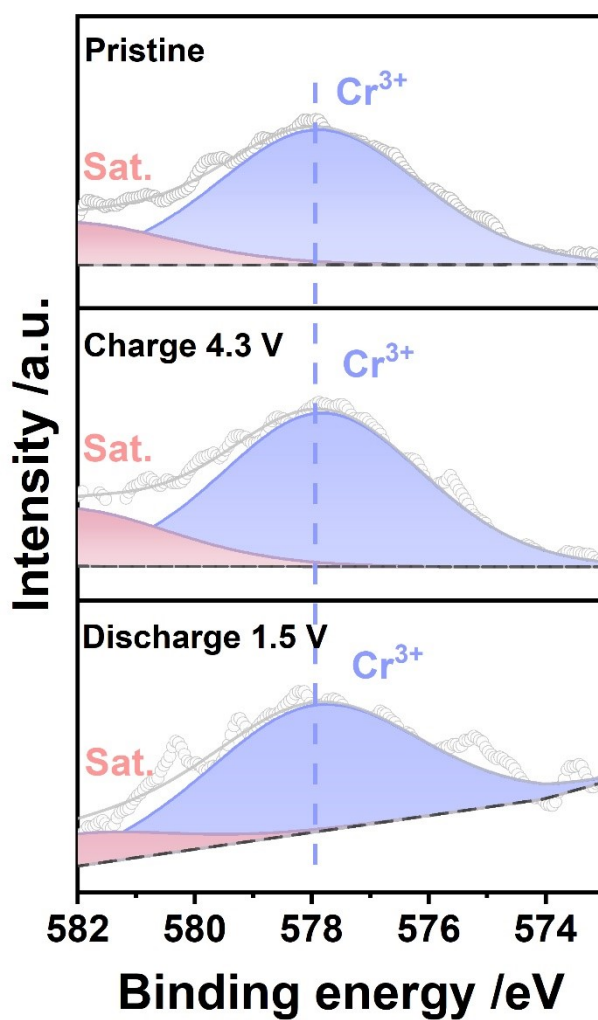
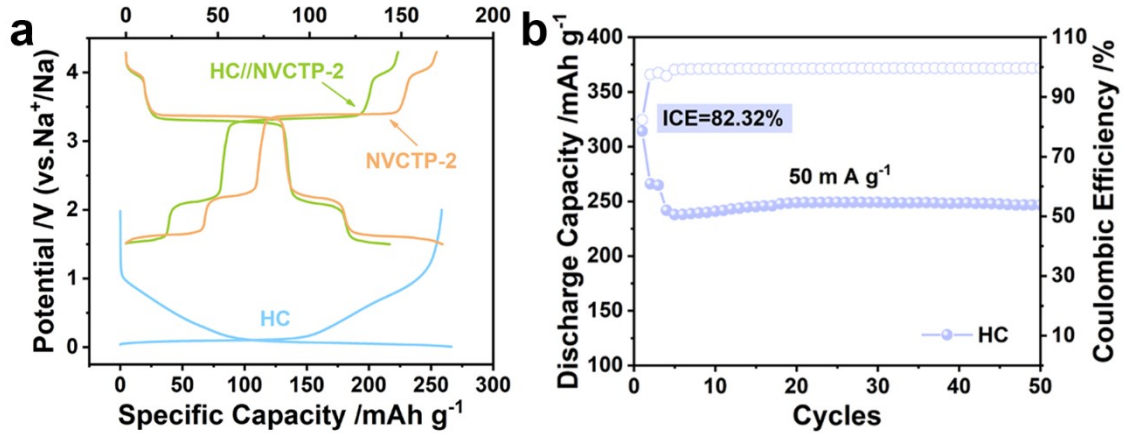
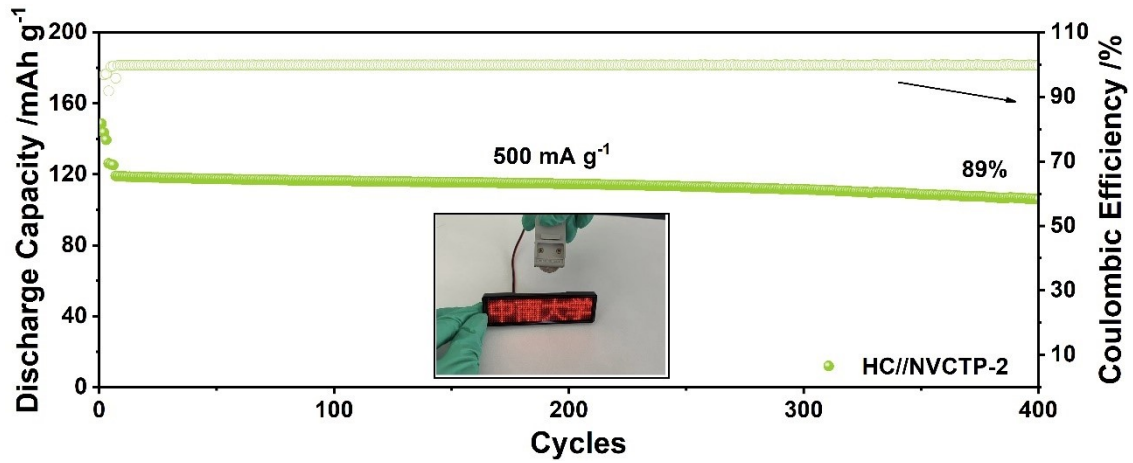


Fig. S14. Ex-situ XPS spectra of Cr  $2p_{3/2}$  for NVCTP-2.



**Fig. S15.** (a) GCD profiles of NVCTP-2 cathode, HC anode, HC//NVCTP-2 full cell. (b) Long-term cyclability of HC in the voltage range of 0.01-2 V.



**Fig. S16.** Long-term cycling stability of HC//NVCTP-2 at 500 mA g<sup>-1</sup>.

### Calculation process for the $D_{Na^+}$ values through GITT tests:

The diffusion coefficient ( $D_{Na^+}$ ) of the as-prepared cathodes is calculated from the GITT potential profiles using Fick's second law. The calculation formula is as follows:

$$D_{Na} = \frac{4}{\pi\tau} \left( \frac{m_B V_m}{M_B S} \right)^2 \left( \frac{\Delta E_s}{\Delta E_\tau} \right)^2 \quad \left( \tau \ll \frac{l^2}{D_{Na^+}} \right)$$

where  $\tau$  represents the duration of the current pulse;  $m_B$  is the mass loading of the electrode material;  $S$  is the geometric area of the electrode;  $\Delta E_S$  is the quasi-thermodynamic equilibrium potential difference between before and after the current pulse;  $\Delta E_\tau$  is the potential difference during the current pulse;  $V_m$  is the molar volume of the electrode material; and  $M_B$  is the molar mass of the electrode material.

**Table S1.** Rietveld structure information of the NVCTP-0 sample.

Space group=R-3c	Rwp=6.46%			
a(Å)=b(Å)= 8.69323	c(Å)= 21.82872		V(Å <sup>3</sup> )= 1428.634	
α(°)=90	β(°)=90		γ(°)=120	
Atom	x	y	z	frac
Na1	0.333300	0.666700	0.166700	0.8579
Na2	0.666700	0.969951	0.083300	0.5555
V	0.333300	0.666700	0.019775	0.7500
Ti	0.333300	0.666700	0.020030	0.2500
P	-0.043082	0.333300	0.083300	1.0000
O1	0.143080	0.499067	0.080704	1.0000
O2	0.540597	0.842954	-0.025611	1.0000

---

**Table S2.** Rietveld structure information of the NVCTP-2 sample.

Space group=R-3c	Rwp=7.44%			
a(Å)=b(Å)= 8.68402	c(Å)= 21.81703		V(Å <sup>3</sup> )= 1424.846	
α(°)=90	β(°)=90		γ(°)=120	
Atom	x	y	z	frac
Na1	0.33330	0.66670	0.16670	0.7816
Na2	0.66670	0.96103	0.08330	0.6561
V	0.33330	0.66670	0.02122	0.6500
Ti	0.33330	0.66670	0.02004	0.2500
Cr	0.33330	0.66670	0.02122	0.1000
P	-0.04215	0.33330	0.08330	1.0000
O1	0.14572	0.49818	0.07945	1.0000
O2	0.53776	0.84147	-0.02638	1.0000

---

**Table S3.** Rietveld structure information of the NVCTP-4 sample.

Space group=R-3c		Rwp=5.56%		
a(Å)=b(Å)= 8.67127		c(Å)= 21.79682	V(Å <sup>3</sup> )= 1419.350	
α (°)=90		β(°)=90	γ(°)=120	
Atom	x	y	z	frac
Na1	0.33330	0.66670	0.16670	0.8531
Na2	0.66670	0.96422	0.08330	0.6555
V	0.33330	0.66670	0.02100	0.5500
Ti	0.33330	0.66670	0.01941	0.2500
Cr	0.33333	0.66670	0.02040	0.2000
P	-0.04588	0.33330	0.08330	1.0000
O1	0.14436	0.49592	0.07925	0.9962
O2	0.54087	0.84116	-0.02663	1.0000

**Table S4.** Rietveld structure information of the NVCTP-2 cathode at pristine, 4.3 V and 1.5 V.

State	Rwp (%)	a,b (Å)	c (Å)	V (Å <sup>3</sup> )
Pristine	3.45	8.6796	21.8113	1423.009
4.3 V	8.02	8.5849	21.7851	1390.483
1.5 V	2.42	8.6896	21.8252	1425.899

**Reference:**

- 1 H. Li, T. Jin, X. Chen, Y. Lai, Z. Zhang, W. Bao and L. Jiao, *Adv. Energy Mater.*, 2018, **8**, 1801418.
- 2 J. Lee, S. Park, Y. Park, J. Song, B. Sambandam, V. Mathew, J.-Y. Hwang and J. Kim, *Chem. Eng. J.*, 2021, **422**, 130052.
- 3 B. Xing, J. Ren, P. Hu, W. Luo, B. Mai, H. Cai, J. Wu, X. Wu, X. Chen, Z. Deng, W. Feng and L. Mai, *Small*, 2024, **20**, 2310997.
- 4 K. Wang, X. Huang, T. Zhou, D. Sun, H. Wang and Z. Zhang, *J. Mater. Chem. A*, 2022, **10**, 10625–10637.